A Study of Correlation between Flame Height and Gap Width of an Internal Fire Whirl in a Vertical Shaft with a Single Corner Gap

G.W. Zou

College of Aerospace and Civil Engineering

Harbin Engineering University

Harbin, Heilongjiang, China

and

H.Y. Hung and W.K. Chow*

Research Centre for Fire Engineering

Department of Building Services Engineering

The Hong Kong Polytechnic University

Hong Kong, China

*Corresponding author:

Fax: (852) 2765 7198; Tel: (852) 2766 5843

Email: beelize@polyu.edu.hk; bewkchow@polyu.edu.hk

Postal address: Department of Building Services Engineering, The Hong Kong Polytechnic University, Hunghom, Kowloon, Hong Kong

Abstract

An internal fire whirl (IFW) can be generated by a pool fire burning in a vertical shaft with a single corner gap of appropriate width. In an IFW, the flame height is an important characteristic in terms of fire safety. In this paper, a correlation expression of flame height with the width of the single corner gap was studied using reported experimental data in a 9 m tall vertical shaft model. A pool of gasoline fuel was burnt inside the shaft model to study the characteristics of flame swirling. An IFW was generated for gap widths lying between 0.11 m and 0.66 m when the pool fire was 0.46 m diameter. The flame height was between 2.5 m and 3.2 m. From the experimental observations on flame swirling for different gap widths, coupled with three assumptions on variation of air entrainment velocity with height, an expression relating the flame height and the corner gap width was derived for the IFW using the set of compiled experimental data. The correlation expression obtained would be useful for fire safety design in vertical shafts.

Keywords: Fire whirl; Vertical shaft; Corner gap width; Flame height; Air entrainment

Introduction

Different arrangements to generate an internal fire whirl (IFW), i.e. a fire whirl inside an enclosure, were reported in the literature.[1-10] Attempts were made to understand the characteristics of IFW including fuel consumption rate, flame height, temperature distribution, velocity distribution, and others. Derivation of the relationships of these characteristics with parameters such as pool size constitutes an important part of the development of appropriate fire models or scaling laws.

An angular momentum source is required to produce swirling velocities while entraining air to the flame. These vorticity-driven air movements occur over a wide range of length and velocity scales, and significantly alter the entrainment and combustion dynamics.[11] The flame height of an IFW is large, even up to several times larger than the height of a normal diffusion flame. The burning rate of a pool fire with IFW is affected by the circular motion of the whirl. Therefore, the flame height of IFW depends on parameters such as the circulation and the core radius of the vortex. Correlations of the flame height of IFW with these vortex parameters were investigated[10-14] through theoretical analysis, experiments and numerical simulations using Computational Fluid Dynamics (CFD). There are many types of IFW generated under different physical processes giving different flame lengths.[1,6,15-21]

In a vertical shaft with a single corner gap, the gap width affects generation of fire whirl. The gap width affects the ventilation and hence the air supply rate to the fire, which changes the burning rate. Once the burning rate is changed, ventilation induced by the fire is also changed as a consequence. There is a complex interplay between the flame characteristics in an IFW in a vertical shaft and the gap width. The aim of the present study is to derive a mathematical expression that correlates the flame height with the corner gap width in an IFW. The model of flame height as proposed in this paper was developed based on experimental observations reported in a previous study.[22] As pointed out by Battablia et al.,[11] fire whirls have not been studied adequately either theoretically or experimentally. Very few studies included fire whirl in practical fire hazard assessment.

Summary of Experimental Results in Previous Study

Experimental setup

Experiments on an IFW were carried out[22] in a vertical shaft model of height 9 m and square base of side 2.1 m in a large burning hall in Harbin, Heilongjiang, China. The vertical shaft was constructed by a steel framework with galvanized steel sheets with an open roof as shown in Fig. 1. A vertical gap with adjustable gap width d_g was opened

at one corner of the model. Ambient air was sucked via the gap into the shaft when burning started. Two pieces of 4-mm thick glass sheets each of height 1.5 m were inserted on the front wall of the shaft for observing the flame motion and shape (Fig. 1).

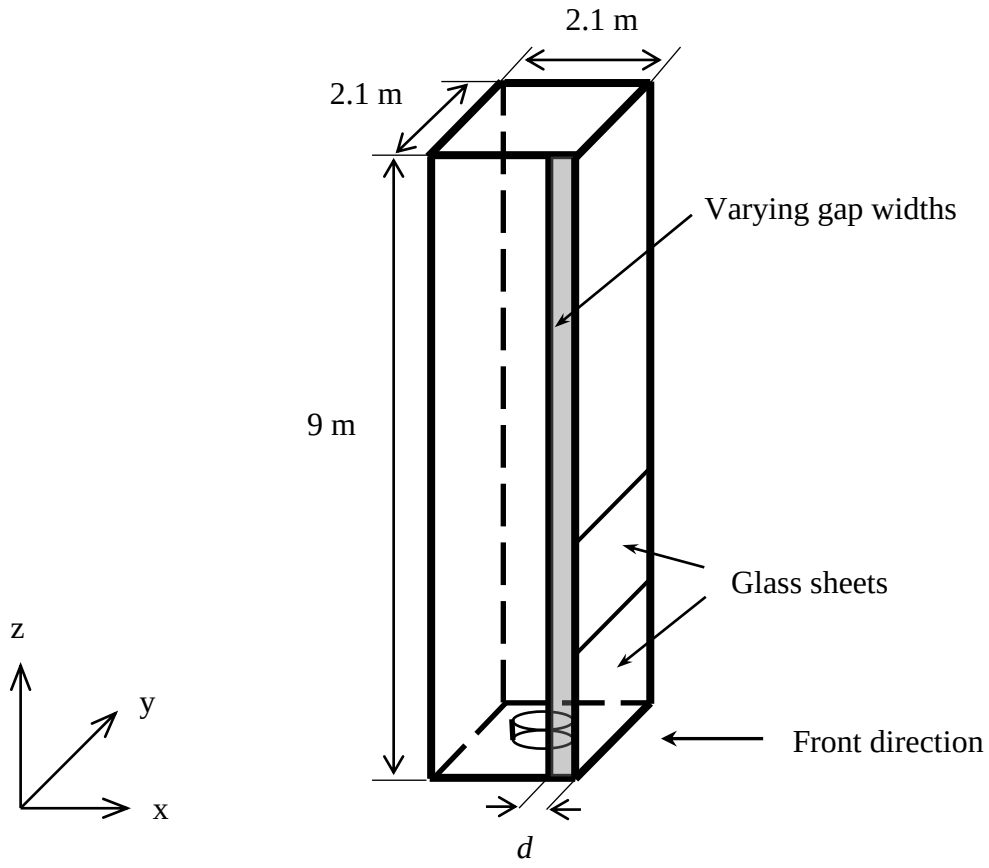

Fig. 1: The vertical shaft model with a single corner gap

A liquid pool fire of tray diameter D equal to 0.46 m was placed at the centre of the base of the shaft model as in Fig. 1. Gasoline 93$^{\#}$ was used as fuel in these experiments.

The physical parameters of gasoline 93# are[23]: heat of combustion 43,070 kJ/kg (10,300 kcal/kg), density from 700 kg/m^3 to 790 kg/m^3, latent heat of vaporization from 290 kJ/kg to 315 kJ/kg, and self-ignition point from 415°C to 530°C.

Experimental Results

Stack effect and wind action in a tall building shaft would affect IFW characteristics and depend on atmospheric conditions. The earlier experiments were carried out[22] in a vertical shaft model of height 9 m inside a large burning hall in summer of Harbin, Heilongjiang, China. Stack effect in the shaft model is not significant. Further, low wind in summer would not bring wind action to the indoor shaft model inside the experimental hall. The ambient temperature and pressure during the test were from 21°C to 24°C and 98510 Pa to 99800 Pa, respectively. Experimental observations indicate that an IFW[22] can be generated by a gasoline pool fire burning in a square vertical shaft model with an open roof and a sidewall corner gap of appropriate width.

For gasoline pool fire burning in free space the flame would take a shape shown in Fig. 2a. The following phenomena were observed when a pool fire burnt in a vertical shaft under different corner gap widths. For burning in the shaft model with no corner gap,

flame did not swirl (Fig. 2b). The flame behaved in a manner similar to a pool fire in free space (Fig. 2a).

(a) Fire in free space (b) Fire in shaft without corner gap (c) Steady internal fire whirl

Fig. 2: Flame shape

When the corner gap width was increased to an appropriate value, a steady fire whirl would be developed (Fig. 2(c)). The formation of IFW follows a sequence of stages consisting of flame tilting, revolution, rotation (or self-spinning) with precession, and eventually IFW formation (Fig. 3(a) through Fig. 3(f)). Note that there is no circular motion in the flame for fire burning in free space.

When the corner gap width was increased further, both flame rotation and precession weakened. The pool fire behaved as that in free space again when the gap width was bigger than a certain value.

For a gasoline fire pool of tray diameter of 0.46 m burning in the 9 m tall shaft model,[22] no swirling motion was observed for corner gap width less than 0.11 m or larger than 0.66 m. Without the formation of IFW, the flame height of the pool fire in the model was about 1.3 m, similar to the flame height for the pool fire in free space. When an IFW was created, the flame height was dependent on the gap width as shown in Table 1. The data were used in the present work for correlational study in the following sections.

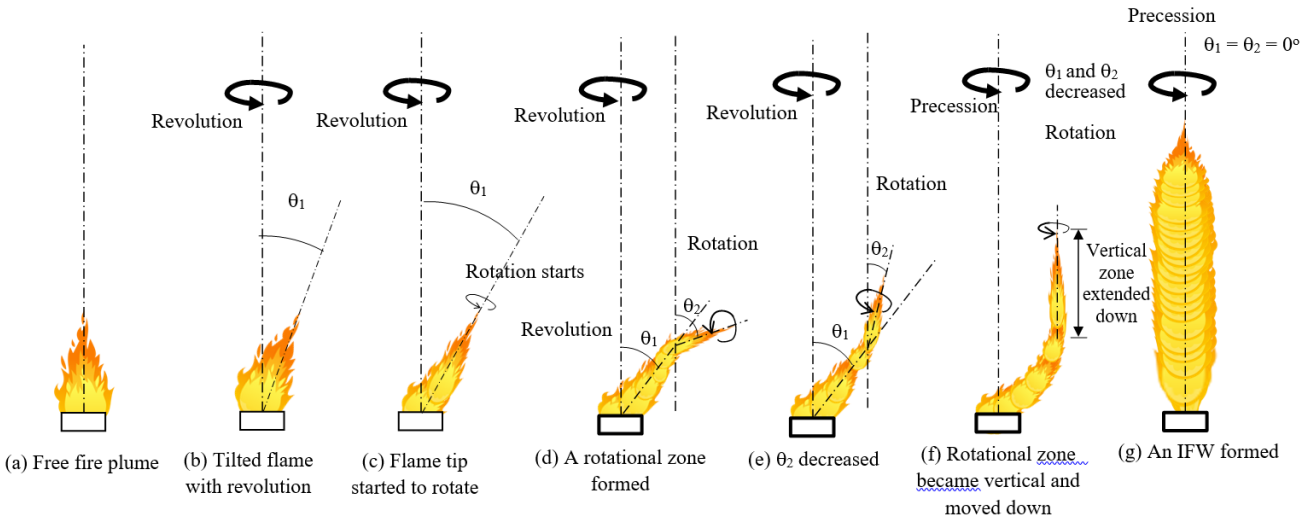

Fig. 3: Stages to form an IFW

Table 1. Flame characteristics corresponding to a pool fire of diameter 0.46 m in a vertical shaft 9 m high and square base of side 2.1 m by Zou and Chow[22]

Vertical gap width d_g [m]	Mean flame height f_h [m]	$d_g^* = \frac{d_g}{a}$	ℓnd^*	$f_h^* = \frac{f_h}{D}$	ℓnf_h^*	Observation on IFW
0.22	2.9	0.1048	-2.2561	6.3043	1.8412	Moderate swirling
0.33	3.2	0.1571	-1.8506	6.9565	1.9397	A clear IFW
0.44	3.1	0.2095	-1.5629	6.7391	1.9079	A clear IFW
0.66	2.9	0.3143	-1.1575	6.3043	1.8412	Moderate swirling
0.88	2.5	0.4190	-0.8698	5.4348	1.6928	Weak swirling

Literature

An IFW generated by a rotating disc surrounded by a fine mesh was reported by Emmons and Ying.[1] A 10 cm-diameter acetone pool fire was placed at the centre of the disc. A buoyancy-driven upward flow was induced by the pool fire. Air passed through the rotating screen to generate swirling motion. Flame height and fuel consumption rates increased with speed of the disc.

IFW experiments were conducted on spinning a 5-cm-diameter methanol pool fire by Chuah et al.[15,16] Vortex flow around the fire whirl was observed to satisfy the continuity and momentum equations with the appropriate boundary conditions. A mathematical

model of Equation (1) was proposed to predict the flame height f_h with a simple scaling analysis:

$$f_h = (f_{h,\infty}^2 + A\frac{r_p^4}{c^2})^{1/2} \quad (1)$$

In the above equation, $f_{h,\infty}$ is the flame height of pool fire without spin, r_p is pool radius (pan radius), c is radius of vortex core and A is a constant.

IFWs generated in square vertical channel with a gap at each corner were studied by Matsuyama et al.,[17], Zhou et al.[18] and Lei et al.[6,19] The temperature distribution of whirling flames, the height of whirling flames, and flow velocity were measured. Different equations were proposed to describe the height of whirling flames.

For heat release rate $\dot{Q}$ of 20 kW, the average flame height H [m] predicted by CFD and experimental data was proposed by Matsuyama et al.[17] in terms of the characteristic fuel size D [m], and the non-dimensional heat release rate $\dot{Q}^*$ as given in Equation (2a):

$$\frac{H}{D} = a_0 + a_1\dot{Q}^{*2/5} \quad (2a)$$

where a_0 and a_1 are constants.

For free burning, the equation is expressed as Equation (2b):

$$H / D = -1.02 + 3.7\dot{Q}^{*2/5} \quad (2b)$$

The average height of whirling flames measured by the experiment was double the values obtained from Equation (2b) for free burning.

The dimensionless form of heat release rate $\dot{Q}^*$ can be evaluated by Equation (2c) in terms of $\dot{Q}$, density of ambient air ρ_∞ (in kgm^{-3}), specific heat capacity $c_{p,\infty}$ (in $kJkg^{-1}K^{-1}$), ambient temperature T_∞ (in K), acceleration of gravity g (in ms^{-2}) and diameter of fuel tray D (in m).

$$\dot{Q}^* = \frac{\dot{Q}}{\rho_\infty c_{p,\infty} T_\infty \sqrt{gD} D^2} \quad (2c)$$

Equations (3) and (4) are the average flame height proposed by Zhou et al.:[18]

$$ln\, H^* = ln\left[\frac{DK(0.37\dot{Q}^*)^m}{H_p}\right] + 2.79m\, ln\, \Gamma^* \quad (3)$$

or

$$H^* = 0.36\Gamma^{*1.11} \quad (4)$$

In Equations (3) and (4), $\dot{Q}^*$ and H_p are respectively the dimensionless heat release rate and the flame height in free burning, $H^* = H / H_p$ is the dimensionless height of whirling flames, D is fuel tray diameter, $\Gamma^* = \Gamma\sqrt{gD^3}$ is the dimensionless circulations, K and m are constants.

Equation (5) is the average flame height proposed by Lei et al.:[6,19]

$$H^* = K(\dot{Q}^* \cdot \Gamma^{*2})^m \quad (5)$$

In Equation (5), $H^* = H / D$ is the dimensionless height of whirling flames, $\dot{Q}^*$ is the dimensionless heat release rate, K is a comprehensive dimensionless quantity and m is a constant.

Steady axi-symmetric strong fire whirls with axes inclined 30° from the vertical orientation were generated by Chuah et al.,[20] in modelling an inclined fire whirl. The rig had six-sided fixed frame wall with two slots. Changes in the velocity profile were assumed to represent a different possible mechanism for extending the flame by

correlating flame characteristics to the strong-vortex approximation and its compensating regime, while accounting for the influence of the viscous core. Equation (6) was proposed by Klimenko and Williams[14] for prediction of the flame height of IFW with a strong rotation obtained by using the compensating regime of vortical flows.

$$L = \frac{F_Z}{\alpha_{\text{eff}} D Z_{\text{st}}} = \frac{u_0 d_0^2}{8\alpha_{\text{eff}} D Z_{\text{st}}} = d_0 \frac{Pe}{8\alpha_{\text{eff}} Z_{\text{st}}} \tag{6}$$

In Equation (6), L is the flame length, α_{eff} is the effective exponent (in the case of a Burgers vortex $\alpha_{\text{eff}} = 2$), D is the diffusion coefficient, Z_{st} is the stoichiometric value of mixture fraction, r_0 is radius at axial location of the fuel source (a pan in experiments), u_0 is the average velocity, $d_0 = 2r_0$, and F_z is the flux of the mixture fraction given by Equation (6a):

$$F_z = \int_0^\infty uZ\rho r \, \mathrm{d}r = \rho_0 u_0 r_0^2 / 2 \tag{6a}$$

Numerical simulation and laboratory experiment were carried out by Zhou and Wu[21] to illustrate that fire whirls can be generated through the interaction between a central flame surrounded by arranged or randomly distributed flames. The effect of rotation speed on the flame height was studied. Equation (7) is a non-dimensional equation

proposed to relate the flame height H to the rotation speed ω through the non-rotating flame height $\overline{H}$ and coefficients L_1 and L_2.

$$H \sim \overline{H} - L_1\omega + L_2\omega^2 \tag{7}$$

As summarized above, there were many studies on fire whirls with different physical conditions and geometry affecting flame heights. However, understanding of the mechanism of fire whirls is still not adequate. At the moment, there is no theory which can explain all the results satisfactorily. No general expression of the whirling flame height has been deduced yet. In view of this, fire whirls generated by a simple vertical shaft model with a single corner gap was studied in this paper.

A fire whirl may be taken as a rotational flow in which combustion drives convection through buoyancy.[12] This convection can be simplified by externally imposed circulation and buoyancy interaction. Assume that the flow is axi-symmetric, steady and inviscid. The steady state Euler equations for a perfect gas in the low Mach number limit would give a tractable model with minimal complexity.

In this study, the Boussinesq model was formulated first, and then the Boussinesq constraint was relaxed by incorporating large density variations. The non-dimensional

form of the governing equations and the boundary conditions were formulated. Results for a buoyant plume with and without swirl were then obtained. The section begins with a description of how the plume changes when subjected to different levels of circulation. The differences in plume development using the Boussinesq model and non-Boussinesq model were contrasted.

The stream function equation was solved numerically with appropriate boundary and initial conditions. The equations were discretized using second-order finite differencing for a standard grid formulation. The form of equation was a modified Poisson equation. To facilitate a solution, a pseudo-time implicit discretization scheme was implemented. The domain for the calculations has dimensions $4r_0 \times 20r_0$, for the radial and axial directions, respectively. Due to regions of high gradients, especially near the centreline, a fine grid was used for simulation, giving a total of 256×1024 cells.

Analytical Study

For an IFW generated as in Fig. 3g, the radial pressure gradient was reduced due to the centrifugal force of circular motion. The vorticity-driven flow would keep the cylinder shape of fire relatively stable in space and time, giving laminar flow to the fire whirl. That means the radial turbulent pulsation of the fire whirl would be greatly reduced. The

flame was similar to laminar diffusion flame with an inner fuel-rich zone and an outer air zone separated by a relatively smooth and stable flame surface. Air surrounding the flame was separated by the stable flame, showing typical characteristics of a diffusion flame. As the radial air entrainment of the fire whirl flame was reduced, the fuel-rich region of the fire whirl moved upward to mix with air. Therefore, a flame with a high height-to-diameter ratio was formed.

For a normal pool fire of which the fuel and the pool surface have equal area with air entrainment available from all sides, a high flame engulfment rate at the radial direction for a pool fire would be higher than that of fire whirl. Hence, the flame diameter of the pool fire would be larger than that of the fire whirl.

The flame of an IFW as formed in Fig. 3g can be taken as a high-speed rotating cylindrical diffusion flame as shown in Fig. 4. Based on this observed pattern, an axis of symmetry was formed along the vertical centreline with air entrained horizontally from all directions.

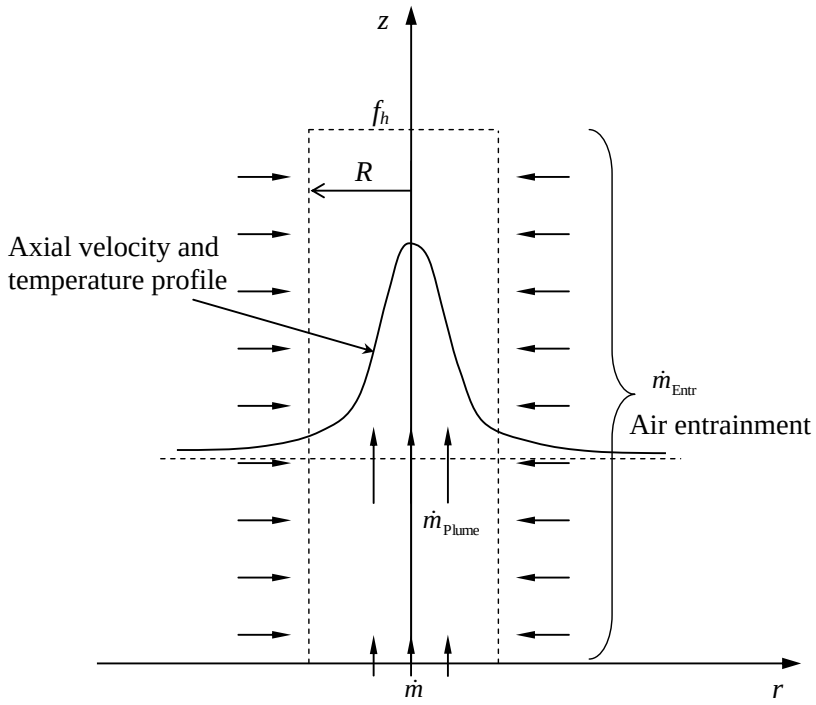

Fig. 4: High-speed rotating cylindrical diffusion plume of fire whirl

An IFW is a complex three-dimensional flow field and the surface of the flame has a helical structure. Within an average time, the flow field of the fire whirl can be taken as axi-symmetric.

Compared to a normal pool fire, the flame surface of an IFW is relatively stable without having large-scale eddies and low buoyancy. Centrifugal force and density gradient along the radial direction would give a stable condition. The flame surface of the IFW is smoother due to the stratification effect of turbulent flame. Mixing and burning of fuel

and air would reduce the flame diameter of fire whirl $R(z)$ axially, and then further reduced to the centre axis at the top part of the fire. However, the change in flame diameter is small in a fire whirl with a tall axial height. Hence the flame diameter $R(z)$ was assumed to be a constant *R*.

Similar to a turbulent fire plume, an IFW has different regions along the axial direction with different radius. Three zones were also observed for the IFW generated in the square vertical shaft with a sidewall corner gap as reported before.[22] Flame pictures observed from the experiments suggested that IFW can be assumed to be high-speed rotating cylindrical diffusion flame. Based on this observation, an axis of symmetry was taken along the vertical centreline with air entrained horizontally from all directions. This is only a simple approximation for easier mathematical analysis. More accurate results can be derived with additional assumptions. However, simple analytical expressions would be difficult and would require more experimental data.

The buoyant axi-symmetric plume mass flow rate $\dot{m}_{\text{Plume}}$ (in kg/s) at some height z above the fuel source in cylindrical coordinates (r,θ,z) can be derived as given in Equation (8), in terms of density ρ, axial velocity $V_z(z,r)$ and flame radius R.

$$\dot{m}_{\text{Plume}}(z) = \int_0^{\infty} (2\pi r)\rho V_z(z,r)\,\mathrm{d}r \approx \int_0^{R} (2\pi r)\rho V_z(z,r)\,\mathrm{d}r \tag{8}$$

The plume mass flow would be increased steadily with height, since ambient air is continually entrained over the plume height. This mass consists of a mixture of combustion products and ambient air would be entrained into the plume, with most of the mass from the ambient air entrained and only a small portion from the combustion products. The plume mass flow rate at the mean flame height f_h can be derived by Equation (9) as a sum of the burning rate $\dot{m}$ and the total air entrainment rate $\dot{m}_{\text{Entr}}$:

$$\dot{m}_{\text{Plume}}(z)\big|_{z=f_h} = \dot{m} + \dot{m}_{\text{Entr}} \approx \dot{m}_{\text{Entr}} \tag{9}$$

With $\dot{m}_{\text{Entr}}$ is given by Equations (10a) and (10b):

$$\dot{m}_{\text{Entr}} = \int_0^{f_h} \frac{\mathrm{d}\dot{m}_{\text{Plume}}}{\mathrm{d}z}\,\mathrm{d}z \tag{10a}$$

or

$$\dot{m}_{\text{Entr}} = \int_0^{f_h} \frac{\mathrm{d}}{\mathrm{d}z}\left[\int_0^{R} \rho V_z (2\pi r)\,\mathrm{d}r\right]\mathrm{d}z \tag{10b}$$

In this vertical shaft model, the rotation of buoyant flame above a gasoline pool is induced by incoming tangential airflow from a sidewall corner gap. The total air

entrainment rate can be determined by Equation (11) in terms of the air velocity at corner gap $V_d(z)$ and the width of sidewall corner gap d_g.

$$\dot{m}_{\text{Entr}} = \int_0^{f_h} d_g \rho_\infty V_d \, \text{d}z \tag{11}$$

Equation (12) is the general form of the combustion reaction.

$$\nu_{\text{Fuel}} \text{ Fuel} + \nu_{\text{Air}} \text{ Air} \rightarrow \sum_i \nu_{\text{Pro},i} \text{ Products} \tag{12}$$

The numbers ν_i are the stoichiometric coefficients for the overall combustion process in which fuel reacts with air (oxygen) to produce a number of products. The stoichiometric Equation (12) implies that the mass consumption rates for fuel and oxidizer per unit volume ($\dot{m}'''_{\text{Fuel}}$ and $\dot{m}'''_{\text{Air}}$) are related to the molecular weights M_{Fuel} and M_{Air} as described by Equation (13).

$$\frac{\dot{m}'''_{\text{Fuel}}}{\nu_{\text{Fuel}} M_{\text{Fuel}}} = \frac{\dot{m}'''_{\text{Air}}}{\nu_{\text{Air}} M_{\text{Air}}} \tag{13}$$

The stoichiometric air-fuel ratio *s* is defined by Equation (14) as:

$$s = \frac{\nu_{\text{Air}} M_{\text{Air}}}{\nu_{\text{Fuel}} M_{\text{Fuel}}} \tag{14}$$

Assuming that a constant proportion γ of entrained fresh air would react with fuel in flame, the burning rate $\dot{m}$ (in kg/s) can be determined by Equation (15) as:

$$\dot{m} = \frac{\gamma \dot{m}_{\text{Entr}}}{s} \tag{15}$$

If the burning rate $\dot{m}$ and effective heat of combustion $\Delta H_{\text{c, eff}}$ are known, the heat release rate $\dot{Q}$ (in kW) of a pool fire can be calculated[23] by Equation (16):

$$\dot{Q} = \dot{m} \Delta H_{\text{c, eff}} (1 - e^{-k\beta D}) \tag{16a}$$

Substituting Equation (15) into Equation (16a), $\dot{Q}$ can be evaluated by Equation (16b) or (16c).

$$\dot{Q} = \frac{\gamma}{s} \dot{m}_{\text{Entr}} \Delta H_{\text{c, eff}} (1 - e^{-k\beta D}) \tag{16b}$$

or

$$\dot{Q} = \frac{\gamma}{s} \Delta H_{\text{c, eff}} (1 - e^{-k\beta D}) d_g \rho_\infty \int_0^{f_h} V_d \, \text{dz} \tag{16c}$$

If the distribution of the velocity $V_d(z)$ is known, then the relation between heat release rate $\dot{Q}$, width of corner gap d_g and flame height f_h can be estimated. Several assumptions were made and justified in the following section.

Although the combustion of an IFW is very fast, the gas-production rate of liquid fuel combustion is much smaller than air entrainment rate and can be neglected. In comparing with the free plume for burning a gasoline pool fire in open space, plume mass flow rate of the gasoline pool fire in this test was calculated to be about 3.51 kg/s. Burning rate of the gasoline pool fire of diameter 0.46 m is 0.0029 kg/s. Therefore, the burning rate of gasoline pool fire burning in open air is much lower than plume mass flow rate. For the developed IFW[22] of diameter 0.46 m, the fuel consumption rate increased to 0.0192 kg/s, which is still less than 3.51 kg/s for a free plume. The fire whirl has a strong entrainment effect to draw much more ambient air than a free plume. Therefore, burning rate of fuel in an IFW is much less than the air entrainment rate for a stable IFW.

Further, the dimensional heat release rate (mass burning rate) was assumed to be unchanged with gap distance. From the earlier results, [22] transient burning duration and the mean flame height of the IFW were roughly the same when sidewall corner width was lying between 0.3 and 0.5 m. The burning duration was about 190 s to 210 s when

an IFW was created. This change is very small compared to the burning duration in open air. It is acceptable to assume the mass burning rate to be unchanged with gap distance when a strong IFW was generated.

Air Entrainment Velocity

Three models of air entrainment, corresponding to three different assumptions on variation of air entrainment velocity along the radial direction V_d with height z, were considered in this study. The first model as given in Equation (17), take V_d as a constant up to the flame height f_h and then at zero above that:

$$V_d = \begin{cases} V_0 & z \le f_h \\ 0 & z > f_h \end{cases} \tag{17}$$

Substituting Equation (17) into Equation (16c), $\dot{Q}$ can be determined by Equation (18) in terms of the fuel tray diameter D (in m), corner gap width d_g (in m), empirical constant $k\beta$ (m^{-1}), mean flame height f_h (in m), effective heat of combustion $\Delta H_{c,\text{eff}}$ (in $kJkg^{-1}$), ρ_∞, constant air velocity at corner gap V_0 (in ms^{-1}), constant proportion entrained fresh air which reacts with fuel γ, stoichiometric air-fuel ratio s.

$$\dot{Q} = \frac{\gamma}{s} V_0 \rho_\infty \Delta H_{c,\text{eff}} (1 - e^{-k\beta D}) f_h d_g \tag{18}$$

A dimensionless flame height f_h^* (in terms of D), and a dimensionless gap width d_g^* (in terms of vertical shaft width a) are respectively defined by Equations (19a) and (19b).

$$f_h^* = \frac{f_h}{D} \tag{19a}$$

$$d_g^* = \frac{d_g}{a} \tag{19b}$$

Then Equation (20) can be derived for determination of $\dot{Q}^*$.

$$\dot{Q}^* = K_2 f_h^* d^* \tag{20}$$

where K_1 is a constant given by Equation (21).

$$K_1 = V_0 a D \frac{\gamma}{s} \frac{\Delta H_{c,\text{eff}} (1 - e^{-k\beta D})}{c_{p,\infty} T_\infty \sqrt{gD} D^2} \tag{21}$$

Assume $\dot{Q}^*$ is constant once an IFW with vigorous swirling is generated. Then Equations (22a) and (22b) can be applied.

$$f_h^* d_g^* = \text{constant} \tag{22a}$$

or

$$\ell n f_h^* + \ell n d_g^{\ *} = \text{constant} \tag{22b}$$

The second model assumes that V_d is constant below the flame height but varies with $1/z^{\alpha_1}$ at height z above the flame height as given in Equation (23).

$$V_d = \begin{cases} V_0 & z \le f_h \\ \dfrac{V_0}{z^{\alpha_1}} & z > f_h \end{cases} \tag{23}$$

The heat release rate can be defined by Equation (24);

$$\dot{Q} = \begin{cases} \dfrac{\gamma}{s}\rho_\infty \Delta H_{\text{c, eff}}(1-e^{-k\beta D})V_0 f_h d_g & z \le f_h \\ \dfrac{\gamma}{s}\rho_\infty \Delta H_{\text{c, eff}}(1-e^{-k\beta D})\dfrac{V_0}{1-\alpha_1} f_h^{\ (1-\alpha_1)} d_g & z > f_h \end{cases} \tag{24}$$

and in Equation (25) in dimensionless form.

$$\dot{Q}^* = \begin{cases} K_1 f_h^* d_g^{\ *} & \dfrac{z}{D} \le f_h^* \\ K_2 (f_h^*)^{1-\alpha_1} d_g^{\ *} & \dfrac{z}{D} > f_h^* \end{cases} \tag{25}$$

where K_2 is a constant given by Equation (26).

$$K_2 = \frac{V_0}{1-\alpha_1} a D^{(1-\alpha_1)} \frac{\gamma}{s} \frac{\Delta H_{c,\text{eff}} (1 - e^{-k\beta D})}{c_{p,\infty} T_\infty \sqrt{gD} D^2} = \frac{D^{-\alpha_1}}{1-\alpha_1} K_1 \tag{26}$$

Assume $\dot{Q}^*$ is constant once an IFW was generated as given in Equation (27). Then $f_h^* d_g^*$ is constant with a relation similar to Equation (22b):

$$\begin{cases} \ell n f_h^* + \ell n d_g^* = \text{constant} & \frac{z}{D} \le f_h^* \\ (1-\alpha_1) \ell n f_h^* + \ell n d_g^* = \text{constant} & \frac{z}{D} > f_h^* \end{cases} \tag{27}$$

The third model of Equation (27) assumes that V_d is proportional to power α_3 of z (z^{α_3}) as in studying wind effects,[6] though there is no clear theoretical basis:

$$V_d = A z^{\alpha_3} \tag{28}$$

The heat release rate can be determined by Equation (29);

$$\dot{Q} = \frac{\gamma A}{s(\alpha_3 + 1)} \rho_\infty \Delta H_{c,\text{eff}} (1 - e^{-k\beta D}) f_h^{\alpha_3 + 1} d_g \tag{29}$$

and Equation (30) in dimensionless form.

$$\dot{Q}^* = K_3 (f_h^*)^{\alpha_3+1} d_g^* \tag{30}$$

where K_3 is a constant as given by Equation (31).

$$K_3 = \frac{AaD^{\alpha_3+1}}{\alpha_3+1} \frac{\gamma}{s} \frac{\Delta H_{\text{c, eff}} (1 - e^{-k\beta D})}{c_{p,\infty} T_\infty \sqrt{gD} D^2} \tag{31}$$

Assume $\dot{Q}^*$ is constant once an IFW is generated. Then Equation (32) is derived.

$$(\alpha_3 + 1) \ell n f_h^* + \ell n d_g^* = \text{constant} \tag{32}$$

Under the three different models or assumptions described above, Equation (33) is obtained:

$$\alpha \, \ell n f_h^* + \ell n d_g^* = \text{constant} \tag{33}$$

where α is a constant.

In all three models for air entrainment proposed above, the plot of $\ell n f_h^*$ against $\ell n d_g^*$ should give a straight line if an IFW is created. However, no IFW was observed if d_g is too large or too small (gap too wide or too narrow). Thus another assumption based on physical observation would be needed.

Correlation between Flame Height and Corner Gap Width

The flame height f_h can be estimated from Equation (16c), if the velocity distribution $V_d(z)$ is known. However, the detailed distribution of the velocity $V_d(z)$ is difficult to determine accurately from experiment. In view of this and also due to limitation in resources, $V_d(z)$ was not measured in this study. Rather, the computational fluid dynamics (CFD) software, Fire Dynamics Simulator (FDS),[24,25] was used to determine $V_d(z)$ the vertical shaft model as shown in Fig. 1. A gasoline pool fire of tray diameter 0.46 m and sidewall corner gap 0.35 m was simulated. Grid distribution is shown in Fig. 5, the size of coarse mesh was 5.0 cm, and that of fine mesh was 2.5 cm.

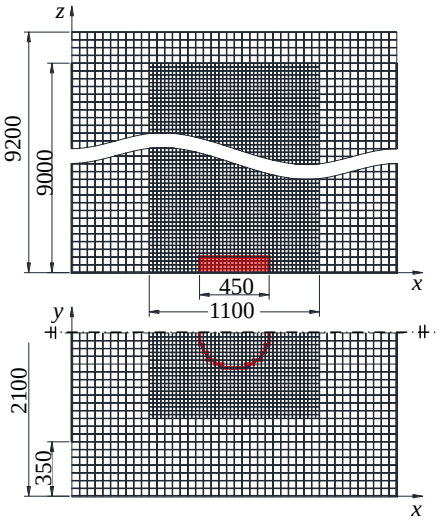

Fig. 5: Grid distribution in FDS for a gasoline pool fire of tray diameter 0.46 m and sidewall corner gap 0.35 m

A mixture fraction combustion model is incorporated in the FDS. The model assumes that combustion is mixing-controlled, and that the reaction of fuel and oxygen is infinitely fast.

The parameter of mixture fraction in FDS was used to show air/fuel ratio. The value of the mixture fraction was equal to 1 in a region corresponding to burning of pure fuel while the value equal to 0 corresponds to pure oxidized air was thus generated, leading to a stoichiometric value that is typically very small, less than 0.1.

The flame height could be defined assuming that the tip of the fire is the point where the mixture fraction reaches its stoichiometric value.[14] The mixture fraction level 0.05 in FDS was used to define an iso-surface for a fire in this study. The predicted transient flame heights are shown in Fig. 6. For gasoline pool fire of tray diameter 0.46 m and vertical gap width 0.33 m, the mean flame height predicted by FDS was 3.25 m, which was very close to the experiment result of 3.2 m.

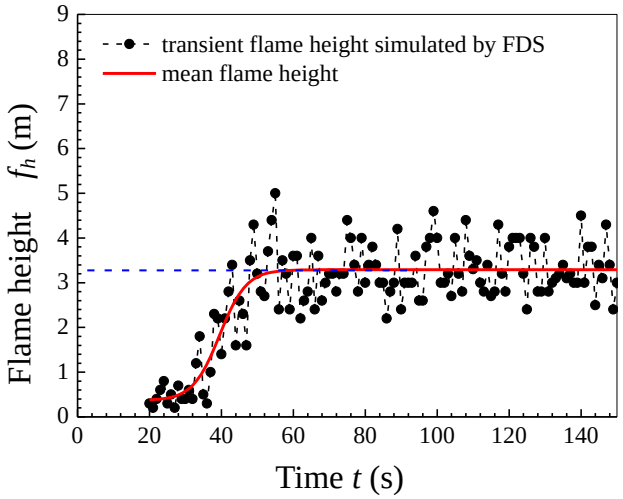

Fig. 6: Flame height simulated by FDS for a gasoline pool fire of tray diameter 0.46 m and sidewall corner gap 0.35 m

Air entrainment velocities along the radial direction $V_d(z)$ predicted by FDS are shown in Fig. 7. As shown in Fig. 7(a), distribution of entrainment velocity at different height along the horizontal direction was uniform. Vertical distribution of velocity at vertical center line of corner gap can be divided into two zones: flame zone and plume zone as

in Fig. 7(b). In the flame zone, the velocity $V_d(z)$ was roughly a constant V_0 for tray diameter 0.46 m and sidewall corner gap 0.35 m.

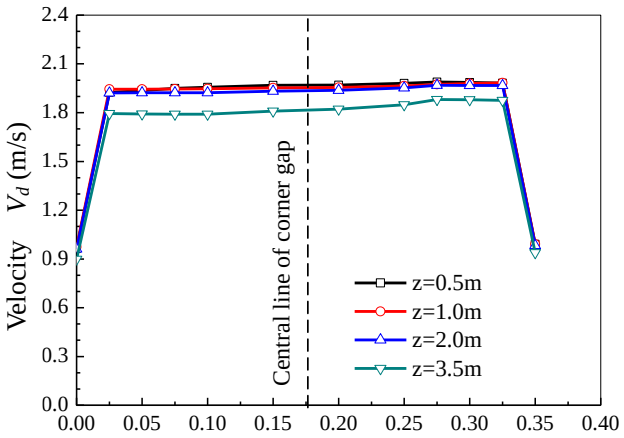

(a) Horizontal distribution of velocity at different height

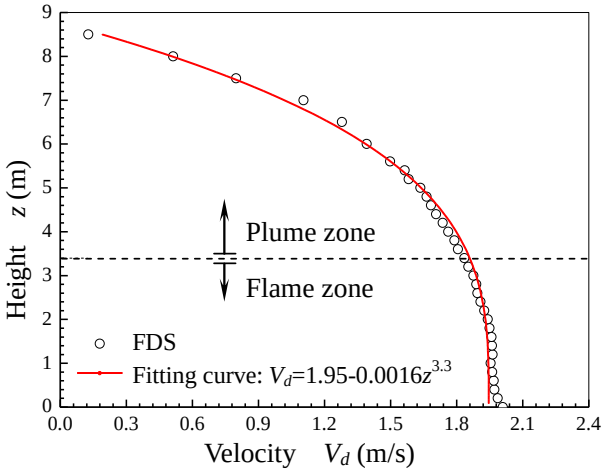

(b) Vertical distribution of velocity at centre line of corner gap

Fig. 7: Air velocity at corner gap induced by fire plume

As shown in Fig. 7(a), distribution of entrainment velocity at different height along the horizontal direction was uniform. Vertical distribution of velocity at vertical centre line of corner gap can be divided into two zones: flame zone and plume zone as in Fig. 7(b). In the flame zone, velocity $V_d(z)$ was roughly a constant V_0 for tray diameter 0.46 m and sidewall corner gap 0.35 m.

The boundary layer effects could still be observed as air speed was very low on both sides of the slit, as shown in Fig. 7(a).

As there was no flame and combustion reaction in the upper smoke zone due to reduction in buoyancy, a reduction in the vertical distribution of velocity at the centre line occurred, as shown in Fig. 7(b).

As observed from experiments[22] in the vertical shaft model, an IFW would be generated only when d_g was lying between a lower limit d_{gl} and an upper limit d_{gu}. Peak flame height was observed at a value d_{go}. Therefore, Equation (34a) is proposed to modify expression (22a) on $f_h^* d_g^*$.

$$f_h^* X = \text{constant} \tag{34a}$$

where X is a dimensionless parameter given by Equation (34b).

$$X = \begin{cases} \dfrac{d_g}{a} & d_{gl} < d_g \le d_{go} \\ \dfrac{2d_{go} - d_g}{a} & d_{go} < d_g \le d_{gu} \end{cases} \tag{34b}$$

Fig. 8 shows the plot of $\ell n f_h^*$ against X for fuel tray diameter D of 0.46 m in the 9-m tall shaft model.[22] A fitted line with correlation coefficient of 0.9995 was obtained, indicating a high degree of correlation as given by Equation (35).

$$\ell n f_h^* = 1.77349 + 0.31187 \ell n X \tag{35}$$

Equation (35) was obtained by line fitting using experimental data from reference.[22] The goodness of fit (high correlation coefficient) shows that the relation between $\ell n f_h^*$ and $\ell n X$ is linear. Thus the linear relation between $\ell n f_h^*$ and $\ell n X$ shown in Equation (34b) was from $\ell n d_g^*$ in Equation (22b) and experimental observation; having a gap width not too narrow nor too wide, as obtained by theoretical analysis, and supported by experimental results.

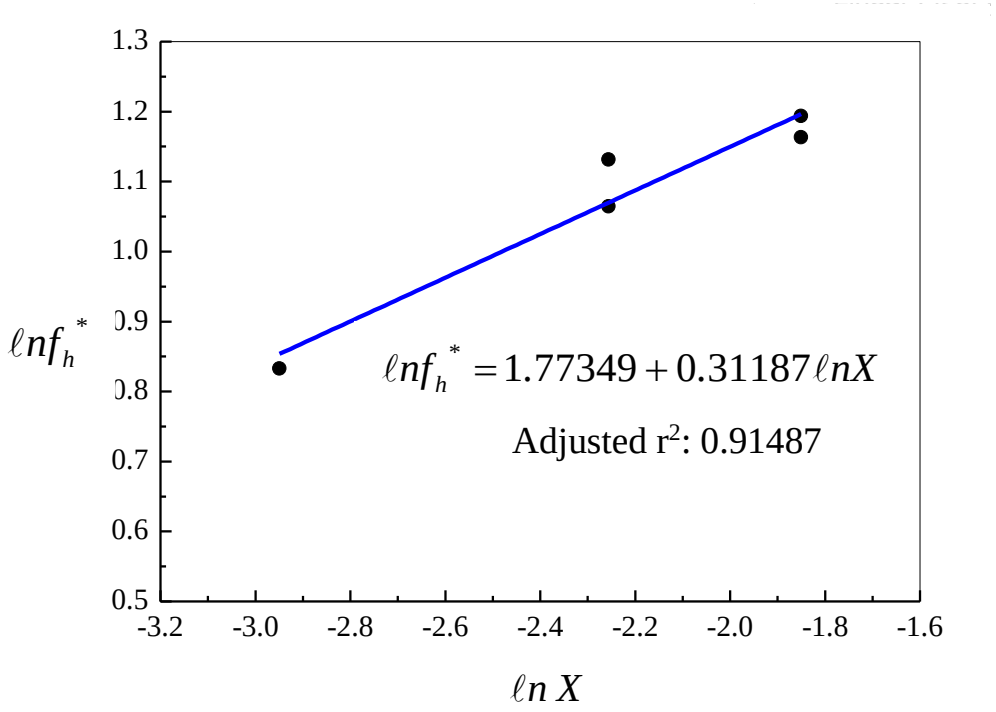

Fig. 8: Correlation of flame height with parameter *X*

If the distribution of the velocity $V_d(z)$ is known (see Equation (16c)), then the relation between heat release rate $\dot{Q}$, width of corner gap d_g and flame height f_h can be estimated without making assumption on velocity. Equation (22a) or Equation (22b) shows a correlation between dimensionless flame height f_h^* and dimensionless corner gap d_g^*.

Experimental data in Fig. 8 were summarized for each test.[22] The data are adequate to determine the correlation expression from experimental observation, pointing out an approach to further study.

Conclusion

Experimental observation on earlier full-scale burning tests indicates that an IFW can be generated by a gasoline pool fire burning in a square vertical shaft model with a single sidewall corner gap with widths lying in an appropriate range. For gap widths wider or narrower than the range, the pool fire either appears as free burning or fire revolution.

Based on our experimentally observed flame swirling and compiled data, coupled with analytical study on vertical distribution of the radial velocity, a correlation of the flame height of an IFW with the corner gap width has been obtained. The results of the present study from experimental observation and theoretical analysis would be valuable in fire safety provision design for vertical shafts in tall green buildings where an IFW might be generated.[26,27]

The model for flame height proposed in this paper was motivated by and originated from experimental observations. In the vertical shaft with a single corner gap, the gap

width was demonstrated to be a key factor in generating fire whirl. There has been no similar study on generating fire whirl in a vertical shaft model with a single corner gap as reported by others. Our analysis has suggested that the approach in deducing correlations can be applied to study similar conditions for other fire whirls in different enclosures for design purpose. Most of the existing models are not for vertical shaft model with a single gap. The present approach is applicable to studies of velocity characteristics. Further studies giving more experimental results and theoretical consideration will be reported in our future papers.

Funding

The work described in this paper was supported by a grant from the Research Grants Council of the Hong Kong Special Administrative Region, China for the project “A study on electric and magnetic effects associated with an internal fire whirl in a vertical shaft” (PolyU 152062/15E) with account number B-Q47D and National Natural Science Foundation of China (No. 51676051).

Declaration

The authors declare that there is no conflict of interest.

Author Contributions

All authors contributed equally in the preparation of this manuscript.

References

1. Emmons HW and Ying SJ. The fire whirl. In: *Proceedings of the 11th International Symposium on Combustion*, 14-20 August 1966, Berkeley, CA. Combustion Institute, Pittsburgh, PA, 1967; pp. 475-488.
2. Satoh K and Yang KT. Experimental observations of swirling fires. In: *Proceedings of the ASME Heat Transfer Division* 1996: International Mechanical Engineering Congress and Exposition, 17-22 November 1996, Atlanta, Georgia. American Society of Mechanical Engineers, 1996; HTD-Vol. 335, Vol. 4: 393-400.
3. Snegirev AY, Marsden JA, Francis J, Makhviladze GM. Numerical studies and experimental observations of whirling flames. *Int J Heat Mass Tran* 2004; 47: 2523-2539.
4. Meroney RN. Fire whirls and building aerodynamics. In: *Proceedings of 11th International Conference on Wind Engineering*, 2-5 June 2003, Texas Tech University, Lubbock, TX; pp. 1-10.

5. Kuwana K, Sekimoto K, Saito K and Williams FA. Scaling fire whirls. *Fire Safety J* 2008; 43: 252-257.
6. Lei J, Liu NA, Zhang LH, Chen HX, Shu LF, Chen P, Deng ZH, Zhu JP, Satoh K and de Ris JL. Experimental research on combustion dynamics of medium-scale fire whirl. *Proc Combust Inst* 2011; 33: 2407-2415.
7. Yang Zifeng, Sarkar Partha and Hu Hui. An experimental study of a high-rise building model in tornado-like winds. *J Fluids Struct* 2011; 27: 471-486.
8. Yu H, Guo S, Peng M, Li Q, Ruan J, Wan W and Chen C. Study on the influence of air-inlet width on fire whirls combustion characteristic. *Procedia Eng* 2013; 62: 813-820.
9. Lei J, Liu N, Lozano JS, Zhang L, Deng Z and Satoh K. Experimental research on flame revolution and precession of fire whirls. *Proc Combust Inst* 2013, 34: 2607-2615.
10. Hayashi Y, Kuwana K, Mogi T and Dobashi R. Influence of vortex parameters on the flame height of a weak fire whirl via heat feedback mechanism. *J Chem Eng Japan* 2013; 46(10): 689-694.
11. Battaglia F, McGrattan K, Rehm RG and Baum HR. Simulating fire whirls. *Combust Theor Model* 2000; 4: 123-138.
12. Battaglia F, Rehm RG and Baum HR. The fluid mechanics of fire whirls: An inviscid model. *Phys Fluids* 2000; 12: 2859-2867.

13. Hayashi Y, Kuwana K and Dobashi R. Influence of vortex structure on fire whirl behavior. *Fire Safety Science* 2011; 10: 671-679.
14. Klimenko AY and Williams FA. On the flame length in fire whirls with strong vorticity. *Combust Flame* 2013; 160: 335-339.
15. Chuah KH and Kushida G. The prediction of flame heights and flame shapes of small fire whirls. *Proc Combust Inst* 2007; 31: 2599-2606.
16. Chuah KH, Kuwana K and Saito K. Modeling a fire whirl generated over a 5-cm-diameter methanol pool fire. *Combust Flame* 2009; 156: 1828-1833.
17. Matsuyama K, Ishikawa N, Tanaka S, Tanaka F, Ohmiya Y and Hayashi Y. Experimental and numerical studies on fire whirls. In: *Proceedings of the 6th Asia-Oceania Symposium on Fire Science and Technology, Daegu, Korea, 17-20 March 2004*. International Association for Fire Safety Science, London, UK, 2004. Session A, Paper 2a-2. http://www.iafss.org/publications/aofst/6/2a-2/view/aofst_6-2a-2.pdf
18. Zhou K, Liu N, Lozano JS, Shan Y, Yao B and Satoh K. Effect of flow circulation on combustion dynamics of fire whirl. *Proc Combust Inst* 2013; 34: 2617-2624.
19. Lei J, Liu N, Zhang L, Deng Z, Akafuah N K, Li T, Saito K and Satoh K. Burning rates of liquid fuels in fire whirls. *Combust Flame* 2012; 159: 2104-2114.
20. Chuah KH, Kuwana K, Saito K, Williams FA. Inclined fire whirls. *Proc Combust Inst* 2011; 33: 2417-2424.

21. Zhou R and Wu ZN. Fire whirls due to surrounding flame sources and the influence of the rotation speed on the flame height. *J Fluid Mech* 2007; 583: 313-345.

22 Chow WK and Han SS. Experimental investigation on onsetting internal fire whirls in a vertical shaft. *J Fire Sci* 2009; 27(6): 529-543.

23 Zou GW, Yang L and Chow WK. Numerical studies on fire whirls in a vertical shaft. In: *Proceedings of 2009 US-EU-China Thermophysics Conference Renewable Energy (UECTC-RE '09)*, Beijing, China, 28-30 May 2009, Paper no. UECTC-RE T10-S20-0419.

24 Chow WK, He Z and Gao Y. Internal fire whirls in a vertical shaft. *J Fire Sci* 2011; 29: 71-92.

25 Chow WK. A study on relationship between burning rate and flame height of internal fire whirls in a vertical shaft model. *J Fire Sci* 2014; 32(1): 72-83.

22. Zou GW and Chow WK. Generation of an internal fire whirl in an open roof vertical shaft model with a single corner gap. *J Fire Sci* 2015; 33(3): 183-201.

23. Iqbal N, Salley MH, Weerakkody S and NRC Project Manager. Fire Dynamics Tools (FDTs): Quantitative fire hazard analysis methods for the U.S. nuclear regulatory commission fire protection inspection program. NUREG-1805, December 2004, Division of System Safety and Analysis, Office of Nuclear Reactor Regulation, U.S. Nuclear Regulatory Commission, Washington DC.

24. McGrattan K, Hostikka S, McDermott R, Floyd J, Weinschenk C and Overholt K. Fire Dynamics Simulator, User's Guide. NIST Special Publication 1019, Sixth Edition. National Institute of Standards and Technology, Gaithersburg, Maryland, USA, and VTT Technical Research Center of Finland, Espoo, Finland, October 2015.
25. McGrattan K, Hostikka S, McDermott R, Floyd J, Weinschenk C and Overholt K. Fire Dynamics Simulator, Technical Reference Guide, Volume 1: Mathematical Model. NIST Special Publication 1018-1, Sixth Edition. National Institute of Standards and Technology, Gaithersburg, Maryland, USA, and VTT Technical Research Center of Finland, Espoo, Finland, October 2015.
26. Chow WK. Performance-based approach to determining fire safety provisions for buildings in the Asia-Oceania Regions. *Build Environ - Fifty Year Anniversary for Building and Environment* 2015; 91: 127-137.
27. Chow WK. Fire hazards of green buildings in the Asia-Oceania regions. Invited talk. *Minisymposium MS94 – "Fire Safety Engineering and Mechanics" in Engineering Mechanics Institute Conference 2017*, San Diego, California, USA, 4-7 June 2017.

IBE_IFWFH3q